

# Synthesis and Electrochemical Behavior of Porous Carbon Powders Prepared by Thermal Plasma Treatment of Phenolic Resin

M. KURIHARA\*, S. MARUYAMA\*, Y. MORIYOSHI\*\*,  
and T. ISHIGAKI\*\*\*

\*TDK Corporation, R & D Center, 113 Nenei, Saku, Nagano 385-8601, Japan,

Fax: 81-267-66-1102, e-mail: Masato\_Kurihara@mb1.tdk.co.jp,

\*\* Hosei University, Department of Materials Science, 3-7-2 Kajino-cho, Koganei, Tokyo 184-0002, Japan,

\*\*\* NIRIM, 1-1 Namiki, Tsukuba, Ibaraki 305-0044, Japan

Carbon powders prepared by the RF thermal plasma treatment of phenolic resin were examined for the anode materials of lithium ion rechargeable battery. Modification of these carbon powders in chemical composition, crystal structure and surface morphology was characteristics of the thermal plasma treatment. The treated powders showed the unique microstructure. TEM observation and micro Raman spectra data showed the non-uniform distribution of graphitized and amorphous areas in a particle. The electrochemical measurements as an anode for lithium ion rechargeable battery were examined in 1M LiClO<sub>4</sub> in a 50:50 mixture of ethylene carbonate and diethyl carbonate. While the electrochemical extraction of lithium ion from plasma-prepared carbon powders proceeded in three stages, the electrochemical insertion looked to proceed in two stages. These electrochemical features can be associated with the uncommon microstructure characteristics.

Key words: carbon, thermal plasma, anode material, lithium ion rechargeable battery,

## 1. INTRODUCTION

Carbonaceous materials have been investigated extensively as an anode material of lithium ion rechargeable batteries by many researchers, in order to obtain high performance such as high capacity, good cycle characteristics and so on. Carbon materials have a various structures from highly ordered graphite to amorphous carbon. Graphite has the theoretical capacity of 372mAh/g, in which lithium content corresponds to that of a graphite intercalation compound (GIC), C<sub>6</sub>Li. It has been reported recently that some kinds of disordered carbonaceous materials have a higher capacity than 372mAh/g [1-5].

Some different mechanisms of lithium storage from the formation of GIC have been proposed to explain the high capacity. Carbonaceous materials derived from polymer precursors heated at low temperature contain some functional groups, such as -C=O, -COOH, -OH and so on. It has been reported hetero atoms, such as hydrogen, nitrogen and oxygen, have an influence on the anode characteristics [4-8]. Also, other authors have proposed a cavity mechanism in which inter-crystallite spaces in carbonaceous material are capable of storing lithium species [3].

Thermal plasma is characterized by its very high temperature (>10,000 K) and high concentration of chemistry reactive species in it. The powders introduced to the plasma are modified in shape, surface morphology, chemical composition and crystal structure in a moment [9]. The present authors have reported the thermal plasma treatment of glassy carbon powder derived from phenolic resin and its electrochemical properties, previously [10]. The plasma treated carbon powder subjected to modifications in chemical composition, morphology on the surface, and graphitization in the bulk, and the modification gave rise to the higher capacity than untreated sample as an anode of lithium ion rechargeable battery. In this work, spherical phenolic resin

powders (novolac type) were treated in induction thermal plasmas with the intention to produce carbon powder directly in a moment, and the electrochemical properties were investigated as an anode for lithium ion rechargeable battery.

## 2. EXPERIMENT

### 2.1 Plasma treatment and characterization

The induction plasma torch and reactor chamber were described elsewhere [11]. Spherical phenolic resin powder (Yunitica, Yunivecs C-50, 27 μm in average particle size) was axially injected into center of the induction thermal plasma with carrier gas. The plasma generating and powder feeding conditions are summarized in Table I. For comparison, ordinal heat treatment of spherical phenolic resin powders were performed at some temperatures (700-1350°C under N<sub>2</sub> atmosphere and 2000-2600°C under vacuum).

Characterization of plasma treated samples were carried out by scanning electron microscopy (SEM), X-ray diffractometry (XRD), the content of carbon, hydrogen, oxygen and nitrogen, Raman scattering spectroscopy and transmission electron microscopy (TEM).

**Table I** Plasma generating and power feeding condition

Sample	A	B	C
Plasma gas flow rates / L · min <sup>-1</sup>			
Plasma gas:	Ar/6	Ar/6	Ar/6
Sheath gas(1):	Ar/30	Ar/30	Ar/30
Sheath gas(2):	H <sub>2</sub> /3	N <sub>2</sub> /3	N <sub>2</sub> /3
Powder carrier gas:	Ar/5	Ar/5	Ar/5
R.F. frequency / MHz	2	2	2
Plate power / kW	40	40	40
Reactor pressure / kPa	53	53	27
Powder feed rate / g · min <sup>-1</sup>	1.3	1.3	2.6

## 2.2 Electrochemical measurements

Sample electrodes were prepared as follows. Polyvinylidene fluoride as a binder, carbon black as a conductive additive and sample powders were mixed in N-methyl-2-pyrrolidone and the slurry was spread on copper foil, and dried at 150°C under vacuum for an hour. A 1 mol·cm<sup>-3</sup> solution of LiClO<sub>4</sub> in a 50:50 mixture of ethylene carbonate (EC) and diethyl carbonate (DEC) was used as an electrolyte. A counter lithium electrode and reference lithium electrode were employed. The electrochemical cells were set up in a dry box under an argon atmosphere and charged/discharged galvanostatically at a current density of 0.25mA·cm<sup>-2</sup> between the limit of 0 to 3V vs. Li/Li<sup>+</sup> at 25°C and 60°C.

## 3. RESULTS

### 3.1 Characterization of plasma-treated powders

The surface of original spherical particles and the heat-treated particles were smooth. The plasma-treated powder remained spherical shape, however the surface was attacked by plasmas and became rough, and fine condensates were formed by coagulation from a vapor phase.

By the plasma treatment in Ar-H<sub>2</sub> and Ar-N<sub>2</sub> plasmas, hydrogen, oxygen and nitrogen contents decreased considerably as shown in Table II. Carbon content in the plasma-treated powder is larger than that in the sample heat-treated at 1100°C, and it is obvious that the spherical phenol resin particles were carbonized by plasma treatment.

The XRD pattern of heat-treated samples and plasma-treated samples are shown in Fig. 1. In the XRD pattern of sample heat-treated at lower temperature (900°C), a broad peak at around 23° indicated that the sample consisted of amorphous structure. In the case of the sample heat-treated at higher temperature (2600°C), there is a main peak at around 26° and the peak top splits into three. The split means the multi-phase graphitization and the crystal structure is still disordered. In the XRD pattern of plasma-treated sample, there are a sharp peak at 26° and a broad peak at 22.5°. This result suggests that the plasma treated powder has a non-uniform structure, which is composed of the graphitized and amorphous structures.

Figure 2 shows typical cross section of plasma-treated sample (sample B) by SEM. The plasma-treated particle is porous and porosity in the central region of particle is higher than that around the surface. The ED pattern around the

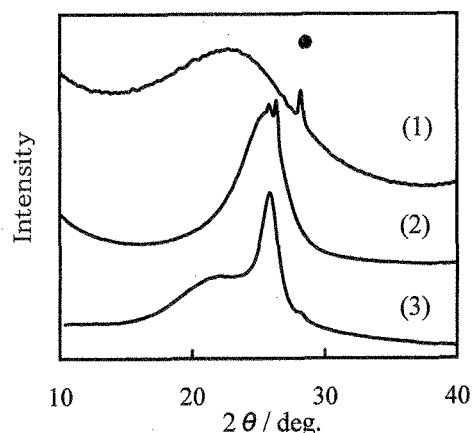


Fig. 1 XRD patterns of (1) sample heat-treated at 900°C, (2) sample heat-treated at 2600°C and (3) plasma-treated sample A (●: from original powder).

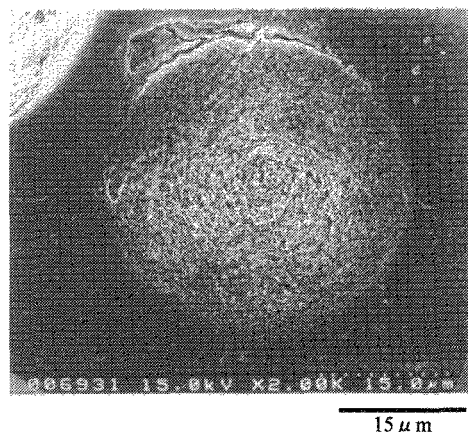


Fig. 2 Typical cross section image of plasma-treated particle by SEM (sample B)

surface of the plasma-treated particle has relatively sharp rings as observed in Fig. 3. On the other hand, the ED pattern in the central region of particle has more obscure rings. This result indicates the crystal structure in the center of particle is more amorphous than that around the surface of particle.

In the Raman spectra of carbon materials, two peaks were observed at about 1580cm<sup>-1</sup> and at about 1350cm<sup>-1</sup>. The 1580cm<sup>-1</sup> band is assigned to the Raman active E<sub>2g2</sub> mode of graphite lattice vibration. The 1350cm<sup>-1</sup> band is originated from the lattice defect, the edge of graphite layers and disordered structure of carbon. Thus, the ratio of the 1580cm<sup>-1</sup> band intensity (I<sub>1580</sub>) and the 1350cm<sup>-1</sup> band intensity (I<sub>1350</sub>), I<sub>1350</sub>/I<sub>1580</sub> (R) can be the indicator of the carbon structure.

In the ordinal, macro-Raman spectra from the surface of the sample particles, the R values of the sample heated at 1100°C, 2600°C, the plasma-treated sample B and C are 1.10, 0.43, 0.60 and 0.57, respectively. It is clear that the plasma treated samples are more graphitized than the sample heated at 1100°C. Since the Raman spectra of carbon materials are restricted to the information from the depth of some tens of nm. Therefore micro-Raman measurement in the cross section of sample particles were performed at intervals of 1 μm from the center to the surface of a particle. Figure 4 shows the R values at each point from the center to the surface in the cross section of

Table II Contents of C, H, O and N in samples

Sample	C/wt%	H/wt%	O/wt%	N/wt%
Phenolic resin	76	18	5	1
Plasma treatment				
A	99.51	0.20	0.25	0.04
B	99.36	0.19	0.33	0.12
C	99.70	0.12	0.12	0.06
Heat treatment				
700°C	97.03	1.24	1.30	0.43
900°C	97.80	0.54	1.15	0.51
1100°C	98.48	0.31	0.82	0.39
1350°C	99.11	0.09	0.48	0.32
2000°C	99.92	0.02	0.04	0.02
2300°C	99.94	0.01	0.04	0.01
2600°C	99.97	0.01	0.01	0.01

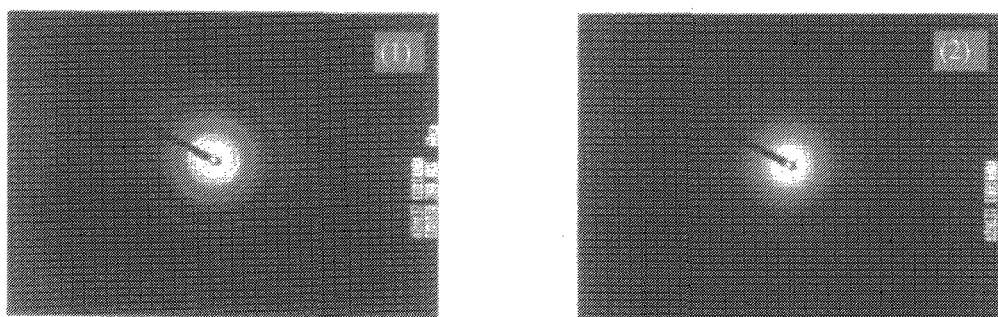


Fig. 3 ED patterns (1) around the surface and (2) in the central region of plasma treated particle (sample C).

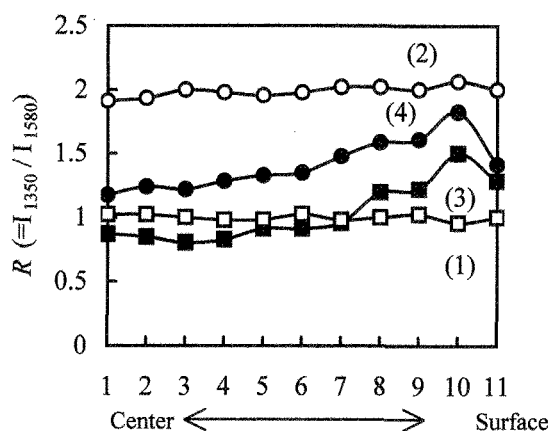


Fig. 4 The relation between the point in the cross section and  $R$  (1) sample heat-treated at 1100°C, (2) sample heat-treated at 2600°C, (3) plasma-treated sample B and (4) plasma-treated sample C

sample particles. The  $R$  value of the heat-treated particles is almost constant at each point in the cross section. The  $R$  value of the sample heated at 2600°C shows relatively high value and higher than that of the sample heated at 1100 °C in Fig.4. It is known that in the Raman spectra from the cross section of highly graphitized samples the  $R$  value can be increased, as the edge of graphite layers appeared remarkably on the cross sectional area of the sample.

In the case of the plasma-treated particles, the  $R$  value around the center, which is close to the value of the sample heated at 1100°C is lower than that around the surface, which is close to the value of the sample heated at 2600°C. This result also shows the plasma-treated particles have non-uniform structure from the center to the surface.

From these results, the plasma-treated particles have non-uniform structure from the center to the surface, that is, the non-uniform distribution of porosity and crystal structure (graphitized and amorphous areas) inside particle.

### 3.2 Electrochemical properties

In the first charging curves of the plasma-treated samples, there is a plateau at about 0.9V with the capacity of about 200 mAh/g. This plateau disappeared in the curves after 2nd cycle. The coulombic efficiency in the first charge/discharge cycle is about 40 %. It is reported that the irreversible capacity of carbon electrode is caused by the film formation on the surface of the electrode and the irreversible capacity is in proportion to the surface area [12]. The plasma treated powders have relatively large surface area (83-95 m<sup>2</sup>·g<sup>-1</sup>). Thus the lower coulombic efficiency in the first

charge/discharge cycle could be explained by this film formation.

Figure. 5(1)-(3) show the second charge/discharge cycling curves of typical heat-treated samples; (1): lower temperature (900°C), (2): higher temperature (2600°C) and (3): typical plasma-treated sample (sample A). In the charge/discharge curve of the sample heat-treated at 900°C (Fig. 5(1)), most of the charge/discharge capacity is shown in the region below 1.0V, and the potential profile does not show any potential plateaus and potential changed gradually in the similar way of the non-graphitizable carbon heated at around 1000°C [4].

In Fig. 5(2), the potential profile does not have clear plateaus associated with the staged structure of highly crystallized graphite [13]. However, more than 75% of the charge/discharge capacity is shown in the potential region lower than 0.3V. The main insertion/extraction of lithium ion into/from graphene layers occurs in this potential region.

The sample heat-treated at 2600°C is the most graphitized in our heat-treated samples, but is less graphitized and more disordered than highly crystallized graphite such as natural graphite (crystallite size  $L_c$  along the  $c$  axis is more than 10000 nm). Because of small crystallite size  $L_c$  along the  $c$  axis (ca. 400 nm), clear plateaus are not observed in Fig. 5(2).

The charge/discharge curve of typical plasma-treated sample shows the characteristics different from the samples heat-treated at lower temperature and at higher temperature as observed in Fig. 5(3). Although the charge curves of plasma-treated samples are similar to the profile of the sample heat-treated at 900°C, the discharge curves differ from that. The charge/discharge curve of the plasma-treated sample is characterized having a large hysteresis and having some potential regions in the discharge curve.

In the potential region below 0.5V, the potential profile is similar to that of the samples heat-treated at 2600°C, in the region between 0.5-1.0V, the potential profile is similar to that of the samples heat-treated at 900°C and in the region above 1.0V, potential changes monotonously and capacity is relatively large (about 100mAh/g). There is a large hysteresis in the equilibrium potential curves obtained by the intermittent charge and discharge. However, discharge capacity does not fade even after 10 cycles.

In the case of the charge/discharge curves of plasma-treated sample at 60°C., both of the charge and discharge capacities at 60°C are larger than those at 25°C, respectively. The discharge capacities below 0.5V at 25°C and at 60°C are almost the same value, on the other hand, the capacity above 1.0V at 60°C is larger than that at 25°C. Moreover, a potential plateau at about 1.0V is observed in the discharge curve at 60°C.

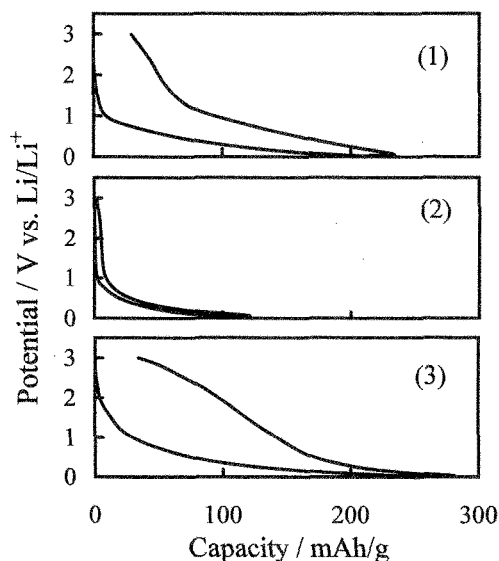


Fig. 5 Second charge/discharge curves of (1) sample heat-treated at 900°C, (2) sample heat-treated at 2600°C and (3) plasma-treated sample (sample A).

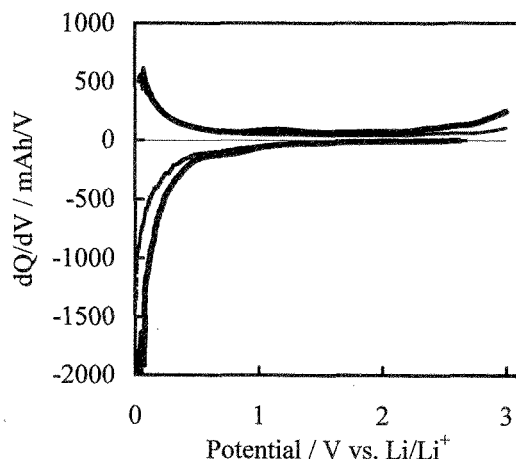


Fig. 6 The differential capacity curve of the plasma-treated sample A (— 25°C, --- 60°C).

In order to display the difference between charge/discharge curves at 25°C and 60°C more clearly, the plot of differential capacity,  $dQ/dV$  against voltage, is given in Fig. 6. A plateau in the charge/discharge curve appears as a peak in the differential capacity curve. The charge capacity at 60°C in the potential region below 0.5V is larger than that at 25°C, however the discharge capacity at 60°C in this region is associated with the lithium insertion site between graphene layers. A peak at 0.9V in charge curve and a peak at 1.1V in discharge peak appear clearly in  $dQ/dV$  curve at 60°C. This couple of peaks corresponds to the potential plateau at about 1.0V in the discharge curves, and the capacity in this plateau suggests the existence of some lithium ion site with the equilibrium potential relatively higher than that of graphite intercalation sites. The feature of  $dQ/dV$  curves of plasma treated sample is the existence of the discharge capacity above 2V in spite of no capacity above 2V in the charge curve. Moreover, the discharge capacity at 60°C above 2V is larger than that at 25°C. In the

charge/discharge curve at 60°C, the extra charge capacity below 0.5V could correspond to the extra discharge capacity above 2V. This result means that a part of lithium ions inserted below 0.5V extracts the potential region above 2V, and suggests the existence of the lithium ion site with relatively large activation energy as reported in case of hydrogen containing carbons obtained by heating of polymers at lower temperature (<800°C) [14]. The unusual behavior would be related to the non-uniform distribution of porosity and crystal structure.

## SUMMARY

The plasma-treated powders have the unique non-uniform distribution of porosity and crystal structure (graphitized and amorphous areas) from the center to the surface inside a particle. Lithium insertion into the plasma treated samples proceeded two stages in the potential areas above 1.0V and below 1.0V, while lithium extraction proceeded three stages in the plateau at around 0.25V, at around 1.0V and the potential area above 2V. These three extraction stages would be identified as (1) extraction from the lithium insertion site between graphene layers, (2) extraction from the site with the equilibrium potential relatively higher than that of graphite intercalation sites and (3) extraction from the site with relatively large activation energy.

## Acknowledgement

This study was performed through Special Condition Funds of the Science and Technology Agency of the Japanese Government.

## REFERENCES

1. K.Sato, M.Noguchi, A.Demachi, N.Oki and M.Endo, *Science*, **264**, 556 (1994).
2. B.M.Way and J.R.Dahn, *J. Electrochem. Soc.*, **141**, 907 (1994).
3. A.Mabuchi, K.Tokumitsu, H.Fujimoto and T.Kasuh, *J. Electrochem. Soc.*, **142**, 1041 (1995).
4. J.R.Dahn, T.Zheng, Y.Liu and J.S.Xue, *Science*, **270**, 590 (1995).
5. F.Disma, L.Aymard, L.Dupont and J.-M.Tarascon, *J. Electrochem. Soc.*, **143**, 3959(1996).
6. Y.Ein-Eli and V.R.Koch, *J. Electrochem. Soc.*, **144**, 2968 (1997).
7. M.Kikuchi, Y.Ikezawa and T.Takamura, *J. Electroanal. Chem.*, **396**, 45 (1995).
8. T.Nakajima and M. Koh, *Denki Kagaku*, **64**, 917 (1996).
9. T.Ishigaki, J.Jurewicz, J.Tanaka, Y.Noriyoshi and M.I.Boulos, *J. Mater. Sci.*, **30**, 883 (1995).
10. M.Kurihara, S.Maruyama, K.Ohe and T.Ishigaki, *Chem. Lett.*, **1998**, 715.
11. T.Ishigaki, Y.Moriyoshi, T.Watanabe and A.Kanzawa, *J. Mater. Res.*, **11**, 2811 (1996).
12. R.Fong, U.von Sacken and J.R.Dahn, *J. Electrochem. Soc.*, **137**, 2009 (1990).
13. T.Ohzuoku, Y.Iwakoshi and K.Sawai, *J. Electrochem. Soc.*, **140**, 2490 (1993).
14. T.Zheng, W.R.MacKinnin and J.R.Dahn, *J. Electrochem. Soc.*, **143**, 2137 (1996).

(Received December 17, 1999 ; Accepted February 15, 2000)